

Connections between RC beam and square tubed-RC column under axial compression: Experiments

Xu-Hong Zhou^{1,2}, Bin-Yang Li^{1,2}, Dan Gan^{*1,2,3}, Jie-Peng Liu^{1,2} and Y. Frank Chen⁴

¹ Key Laboratory of New Technology for Construction of Cities in Mountain Area (Ministry of Education), Chongqing University, Chongqing 400045, China

² School of Civil Engineering, Chongqing University, Chongqing, 40045, China

³ School of Civil Engineering, Chang'an University, Xi'an 710061, China

⁴ Department of Civil Engineering, The Pennsylvania State University, Middletown, PA 17057, USA

(Received August 03, 2016, Revised January 13, 2017, Accepted January 18, 2017)

Abstract. The square tubed-reinforced concrete (TRC) column is a kind of special concrete-filled steel tube (CFST) columns, in which the outer thin-walled steel tube does not pass through the beam-column joint, so that the longitudinal steel reinforcing bars in the RC beam are continuous through the connection zone. However, there is a possible decrease of the axial bearing capacity at the TRC column to RC beam connection due to the discontinuity of the column tube, which is a concern to engineers. 24 connections and 7 square TRC columns were tested under axial compression. The primary parameters considered in the tests are: (1) connection location (corner, exterior and interior); (2) dimensions of RC beam cross section; (3) RC beam type (with or without horizontal haunches); (4) tube type (with or without stiffening ribs). The test results show that all specimens have relatively high load-carrying capacity and satisfactory ductility. With a proper design, the connections exhibit higher axial resistance and better ductility performance than the TRC column. The feasibility of this type of connections is verified.

Keywords: square tubed-reinforced-concrete (TRC); concrete filled tube connections; horizontal haunched RC beam; failure pattern; axial compression behavior

1. Introduction

Concrete-filled steel tube (CFST) has been developed for some time. Due to economy and superior structural behavior, it has been popularly utilized in modern buildings. To eliminate or delay the local buckling of thin steel tubes and promote the practical use of them, a new type of composite columns, named tubed-reinforced-concrete (TRC) column, was proposed (Tomii *et al.* 1985, Liu and Zhou 2010), where the steel tube does not pass through the beam-to-column connection and terminated at the column ends (Fig. 1).

Laboratory tests under axial compression, eccentric compression, and cyclic loading (Sakino and Sun 2000, Han *et al.* 2009, Liu *et al.* 2009 and 2015, Yu *et al.* 2010, Zhou and Liu 2010, Chen *et al.* 2011 and 2012, Wang *et al.* 2015) showed that the square TRC columns, especially those with the stiffened square tube, possessed high load-carrying capacity and good ductility performance. The longitudinal rebars in RC beams can pass through the connection zone freely without interfering with the added steel strengthening ring or steel bracket in the connection zone, thus simplifying the construction process and saving the cost. However, there is a concern from the engineers on the

possible decrease of the axial bearing capacity due to the discontinuity of the column tube.

To prevent the failure at connection, many studies have been performed in past years. Nie *et al.* (2008) and Bai *et al.* (2008) developed a through-beam connection system for concrete-encased CFST columns and RC beams, where multiple lateral hoops and a prefabricated steel cage with cast concrete were used to enhance connection zone. Test results showed with the help of stiffening ring, the “strong joints” design philosophy can be achieved in both axial compression and cyclic loading tests. Zhang *et al.* (2012) investigated the seismic behavior of another type of through-beam connections consisting of a ring beam joint with a discontinuous outer tube between concrete-filled twin steel tubular columns and RC beams. Chen *et al.* (2014, 2015) performed an experimental and analytical study on the seismic and axial compressive behavior of a new type of through-beam connections between CFST columns and RC beams, in which a strengthening RC ring beam was used to enlarge the connection zone. The effects of the ratio of reinforcing ring beams were elucidated through parametric studies done by finite element analysis. It was shown that with a proper design, the through-beam connections exhibited excellent load-carrying capacity and ductility. The researches mentioned above demonstrated that using strengthening RC ring is an effective way to strengthen connection between RC beams and CFST columns.

Recently, the new type of TRC columns was applied at

*Corresponding author, Ph.D.,
E-mail: gandan@cqu.edu.cn

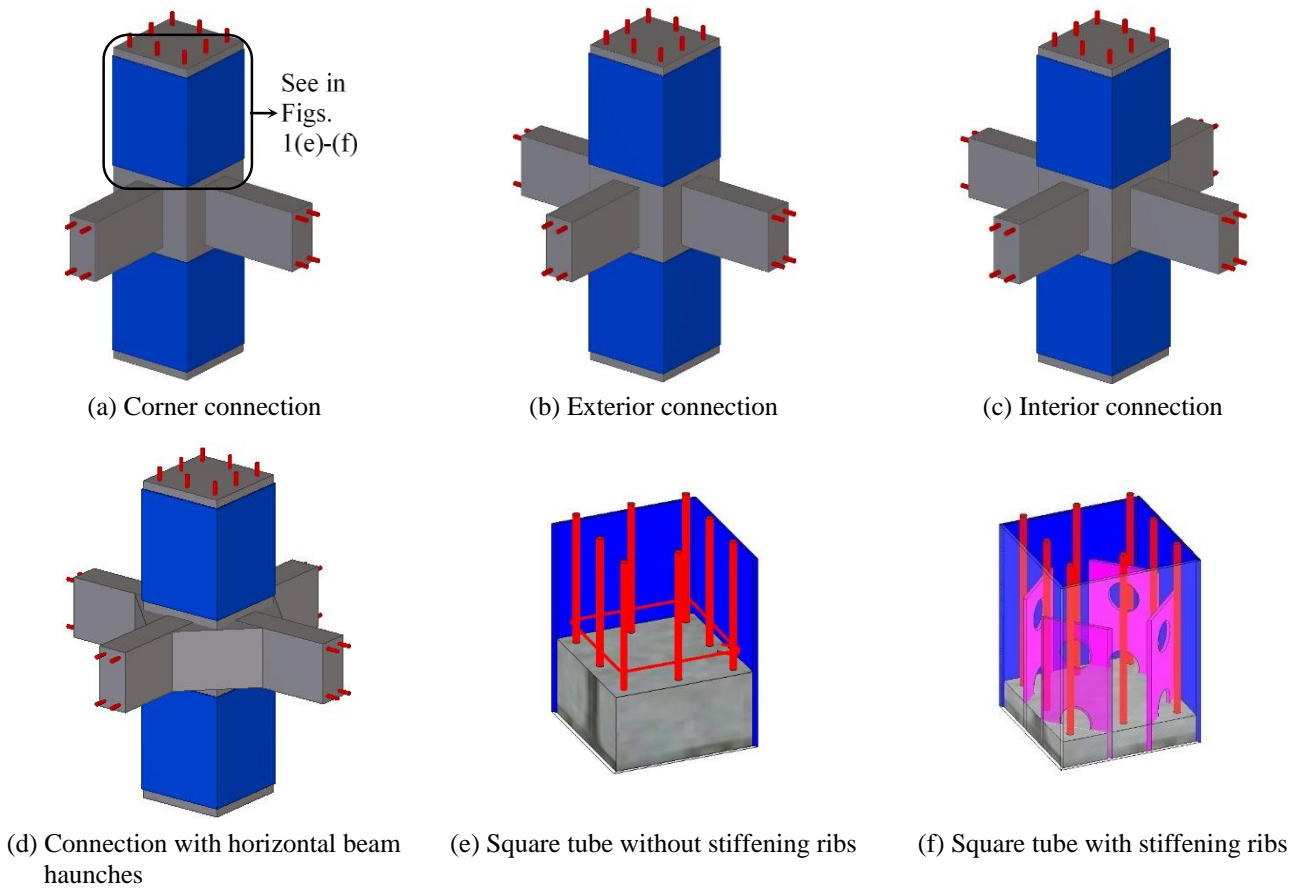


Fig. 1 Square TRC column to RC beam connection



Fig. 2 Practical application of square TRC connection

the basement and the lower three stories of a high-rise building in Harbin, China (Fig. 2). With the increasing use of TRC columns, safety and economical design for the connections between RC beams and TRC columns are required. Contrasting to the connections related to conventional CFT structures, limited research on RC beam-square TRC column connections has been done. Compare with conventional CFST construction, thinner tube can be used in TRC construction (Han *et al.* 2009). Moreover, the beam-column joint of RC beams and TRC columns can be designed without strengthening RC rings. Han *et al.* (2009) investigated the behavior of the composite joints consisting of thin-walled steel tube confined plain concrete column and RC beam under cyclic loading. Their test result show

that without stiffening ring the TRC composite joint still has good seismic performance and may be practically applied to buildings.

This paper discusses the experimental results of 24 RC beam-square TRC column connections and 7 contrastive square TRC columns under axial compression, laying the groundwork for the study of seismic behavior of the connections in a real structure. The primary parameters considered in the tests are: (1) connection location (corner, exterior and interior shown in Figs. 1(a)-(c)); (2) dimensions of RC beam cross section; (3) RC beam type (with or without horizontal haunches) (Fig. 1(d)); and (4) tube type (with or without stiffening ribs) (Figs. 1(e)-(f)).

Table 1 Parameters of the test specimens

Group	Specimen	B (mm)	H (mm)	h (mm)	b (mm)	l (mm)	Stirrups (Joint)	$N_{p,exp}$ (kN)	$\frac{N_{p,exp}}{N_{p,col}}$	$\varepsilon_{p,exp}$ ($\mu\varepsilon$)	$\frac{\varepsilon_{p,exp}}{\varepsilon_{p,col}}$
GS	S(GS)-200-a	200	600	-	-	-	-	3143.2	-	2165	-
	S(GS)-200-b	200	600	-	-	-	-	2623.4	-	3366	-
	SC(GS)-140-2	200	740	140	70	140	D10@50	2952.9	1.02	2658	0.96
	SC(GS)-140-3	200	740	140	70	140	D10@50	-	-	-	-
	SC(GS)-140-4	200	740	140	70	140	D10@50	-	-	-	-
	SC(GS)-180-2	200	780	180	90	180	D10@70	3006.4	1.04	2625	0.95
	SC(GS)-180-3	200	780	180	90	180	D10@70	2907.6	1.01	2421	0.88
	SC(GS)-180-4	200	780	180	90	180	D10@70	3044.6	1.06	3071	1.11
	SC(GS)-140-2-S	200	740	140	70	140	D10@50	3266.7	1.13	3082	1.11
	SC(GS)-140-3-S	200	740	140	70	140	D10@50	3343.9	1.16	3037	1.10
	SC(GS)-140-4-S	200	740	140	70	140	D10@50	3309.3	1.15	3414	1.23
	SC(GS)-180-2-S	200	780	180	90	180	D10@70	3301.9	1.15	4551	1.65
	SC(GS)-180-3-S	200	780	180	90	180	D10@70	3265.7	1.13	5442	1.97
	SC(GS)-180-4-S	200	780	180	90	180	D10@70	3305.4	1.15	3185	1.15
OS	S(OS)-200-a	200	600	-	-	-	-	3250.2	-	3287	-
	S(OS)-200-b	200	600	-	-	-	-	3086.0	-	2649	-
	S(OS)-200-c	200	600	-	-	-	-	3381.0	-	3104	-
	SC(OS)-200-2-H-a	200	600	200	120	120	D10@50	2918.3	0.90	4477	1.49
	SC(OS)-200-2-H-b	200	600	200	120	120	D10@50	3048.1	0.94	2965	0.98
	SC(OS)-200-2-H-c	200	600	200	120	120	D10@50	2902.5	0.90	2682	0.89
	SC(OS)-200-3-H-a	200	600	200	120	160	D10@50	3362.9	1.04	3573	1.19
	SC(OS)-200-3-H-b	200	600	200	120	160	D10@50	3346.0	1.03	3915	1.30
	SC(OS)-200-3-H-c	200	600	200	120	160	D10@50	3140.2	0.97	7905	2.62
	S(OS)-240-a	240	720	-	-	-	-	4090.5	-	3092	-
	S(OS)-240-b	240	720	-	-	-	-	3686.5	-	2790	-
	SC(OS)-240-2-H-a	240	720	240	120	120	D10@50	4144.6	1.07	2841	0.97
	SC(OS)-240-2-H-b	240	720	240	120	120	D10@50	4142.6	1.07	3219	1.09
	SC(OS)-240-2-H-c	240	720	240	120	120	D10@50	4228.1	1.09	3772	1.28
SC(OS)-240-3-H-a	240	720	240	120	160	D10@50	4299.2	1.11	3856	1.31	
SC(OS)-240-3-H-b	240	720	240	120	160	D10@50	4083.9	1.05	3780	1.29	
SC(OS)-240-3-H-c	240	720	240	120	160	D10@50	4256.7	1.09	3148	1.07	

* $N_{p,exp}$: Peak load;* $N_{p,col}$: Average peak load of corresponding columns;* $\varepsilon_{p,exp}$: Peak vertical strain;* $\varepsilon_{p,col}$: Average peak vertical strain of corresponding columns.

Table 2 Material properties of the test specimens

Group	Steel tube		Longitudinal steel bar (column)		Longitudinal steel bar (beam)		Stirrup (Column)		Stirrup (Joint)		Concrete f_{co} (Mpa)
	t (mm)	f_y (Mpa)	d (mm)	f_y (Mpa)	d (mm)	f_y (Mpa)	d (mm)	f_y (Mpa)	d (mm)	f_y (Mpa)	
GS	1.49	314.1	19.12	480.6	9.90	324.8	8.02	316.9	9.90	324.8	45.0
OS	1.50	364.3	19.40	477.1	9.52	549.3	7.91	315.3	9.52	549.3	48.1

Details of the test variables for each specimen are listed in Table 1. Two groups of specimens were designed: Group GS contains no horizontal RC beam haunch, while Group OS contains. The main parameters considered in Group GS

are: (1) connection locations (corner, exterior & interior); (2) beam heights (140 mm & 180 mm); (3) steel tube types (stiffened & unstiffened). The main parameters considered in Group OS are: (1) connection locations (corner &

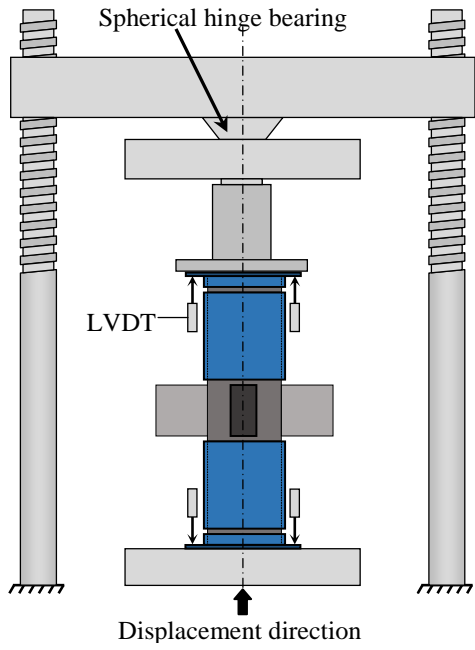


Fig. 4 Testing machine and LVDT arrangement



(d) SC(GS)-180-4-S



(e) SC(GS)-180-2



(a) S(GS)-200-a



(f) SC(GS)-140-2-S



(b) SC(GS)-180-4



(g) SC(GS)-140-3-S



(c) SC(GS)-140-4-S



(h) SC(GS)-180-3-S



Fig. 5 The failure patterns of the specimens in Group GS

Fig. 5 Continued

exterior); (2) width of square column (200 mm & 240 mm); and (3) beam height (200 mm & 240 mm).

The square tubes were cold-formed and welded at the middle. The properties of steel plates and concrete are presented in Table 2 where f_{co} is the average concrete compressive strength of 150 mm × 150 mm × 300 mm prism. For the labeling system of column specimens, the first symbol indicates square TRC column (S) or connection (SC); the second number of column represents the width of square column (B); for the connection, the second number represents the height of beam section (h), the third number (2, 3, or 4) represents corner, exterior or interior connection, the fourth letter designates horizontal RC haunch (H) or stiffened tube (S), and the last letter (a , b , or c) is used to identify the specimen. For examples, S(GS)-200-a represents a square TRC column of Group GS with the width of 200mm and SC(OS)-240-2-H-a represents a corner connection with horizontal RC haunches and 240 mm wide column section.

2.2 Test set-up and instrumentation layout

All specimens were tested using a 5000kN hydraulic compression machine (Fig. 4). Although the boundary conditions of the beams are unconstrained, it would not affect the investigation on the axial compressive behavior of the composite connection as it is usually subjected to a high axial load. As indicated above, current study will provide the groundwork for further studies such as seismic behavior of the connections (Nie *et al.* 2008, Chen *et al.* 2015). The loading rate was at 1-2 kN/s in the elastic range. The compressive load was applied slowly and continuously near and after the peak load in order to investigate the softening behavior of the specimens.

Fig. 4 depicts the instrumentation layout for the speci-

mens. Eight linear variable displacement transducers (LVDT) were used to monitor the axial deformation during the test. Strain gauges were placed on the surfaces of steel tube and concrete to measure the strains in the tube and joint zone (Fig. 2).

3. Test results of Group GS

3.1 Failure patterns

Fig. 5 illustrates the typical failure patterns of the connections and square TRC columns in Group GS. For the square TRC columns, the crushing of concrete along a diagonal section and the buckling of longitudinal reinforcing bars were observed (Fig. 5(a)).

The typical failure pattern of the interior connections in Group GS is shown in Figs. 5(b)-(d). Tube dilation was observed at the mid-height of column zone for both stiffened and unstiffened square tubes. Upon removing the tube after the test, the concrete crushing and steel bar buckling were observed at the location where the tube dilated. The failure pattern of interior connections may be viewed as a column failure.

The typical pattern of the exterior (Figs. 5(e)-(f)) and corner (Figs. 5(g)-(h)) connections is similar to that of the interior connections. However, spalling of the concrete cover at the connections was observed due to the nonexistence of transverse RC beams. As a result, the general failure pattern for all specimens in Group GS is a column failure. The stiffened square tube does not appear to alter the failure pattern.

3.2 Load-deformation relationship

The load (N) versus axial strain (ϵ) curves for the

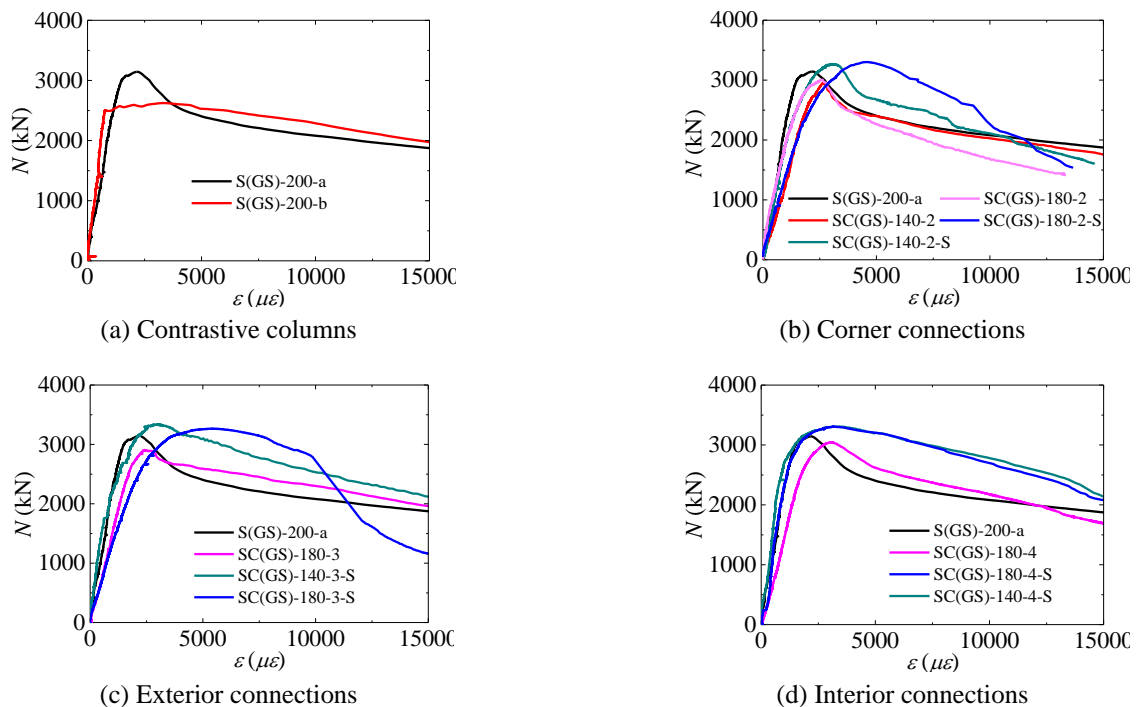
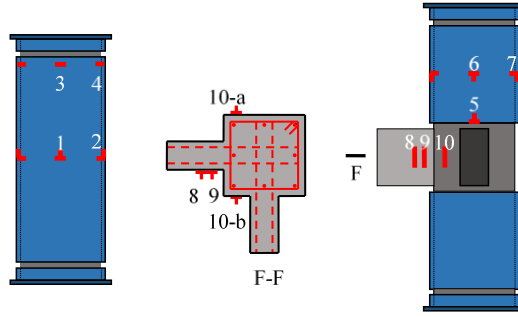
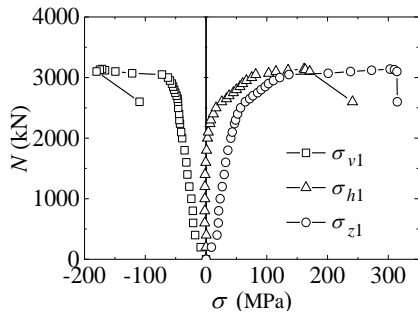


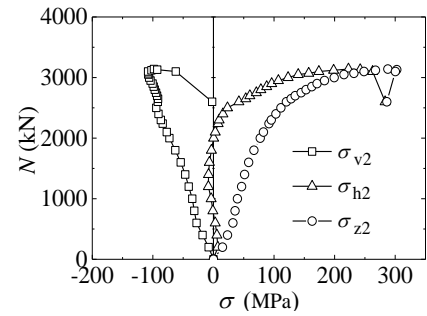
Fig. 6 The load-strain curves of the specimens in Group GS



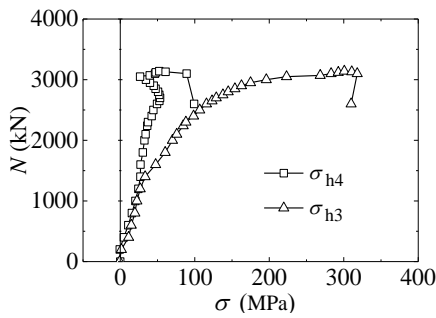
(a) Locations of corresponding strain gauges



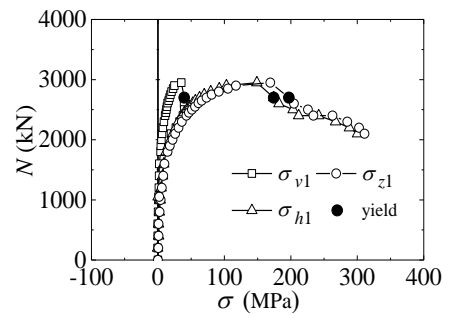
(b) Point 1 of S(GS)-200-a



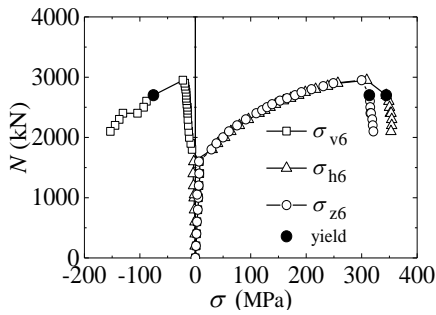
(c) Point 2 of S(GS)-200-a



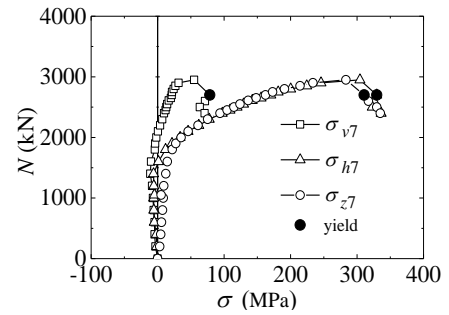
(d) Points 3 and 4 of S(GS)-200-a



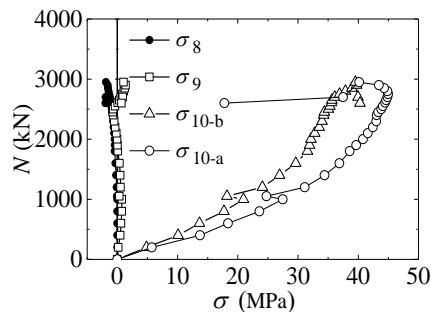
(g) Point 5 of SC(GS)-140-2



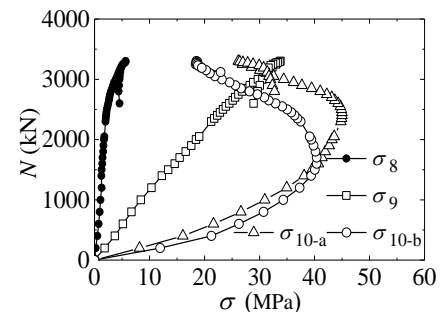
(e) Point 6 of SC(GS)-140-2



(f) Point 7 of SC(GS)-140-2



(h) Points 8 to 10 of SC(GS)-140-2



(i) Points 8 to 10 of SC(GS)-180-2-S

Fig. 7 The load-stress curves of the specimens in Group GS

specimens in Group GS are presented in Fig. 6. The axial strain of specimen is defined as $\epsilon = \Delta/H$, where Δ is the axial displacement and H is the height of the specimen. The test data for SC(GS)-140-3 and SC(GS)-140-4 are not shown in this paper due to the concrete defects in the connection zone associated with the pouring. As indicated, all other specimens exhibit a good strength and satisfactory ductility.

As shown in Figs. 6(a)-(d) and Table 1, the peak loads ($N_{p,exp}$) of the connection specimens without stiffening ribs in Group GS are close to those of the contrastive columns. Due to the steel discontinuity, the peak load of some

connections is slightly lower than that of the contrastive columns (for example, SC(GS)-180-3). However, this will not change the failure mode because the peak load of the joint zone is relatively high compared to the column zone in a same specimen.

The beam height and connection type affect little on bearing capacity, elastic stiffness, and ductility. The stiffening ribs have a significant influence on both peak load and ductility. $N_{p,exp}$ values for the connections with stiffening ribs are 8.6-10.6% higher than those without. The stiffening ribs effectively improve the confinement of square tube as well as the bearing capacity and ductility of



(a) S(OS)-200-a



(b) S(OS)-200-c



(c) SC(OS)-200-3-H-a



(d) SC(OS)-200-3-H-b



(e) SC(OS)-240-3-H-a



(f) SC(OS)-240-3-H-b



(g) SC(OS)-200-2-H-b



(h) SC(OS)-240-2-H-b



Fig. 8 Failure patterns of the specimens in Group OS

Fig. 8 Continued

the connections.

3.3 Load-stress analysis

The elastic-plastic analysis method (Zhang *et al.* 2005) was adopted to analyze the stress condition of the steel tubes based on the measured strains. According to this method, the stress along the tube thickness is small and may be neglected. Therefore, the steel plate can be treated as a plane-stress problem. von Mises yield criterion was thus employed to describe the yielding behavior of the steel. Fig. 7 illustrates the analysis results for typical specimens, in which σ_v and σ_h are longitudinal stress and transverse stress of the steel tube respectively and σ_z is the equivalent stress determined from the following equation

$$\sigma_z = \frac{\sqrt{2}}{2} \sqrt{(\sigma_v - \sigma_h)^2 + \sigma_v^2 + \sigma_h^2} \quad (1)$$

The load-tube stress responses for S(GS)-200-a are presented in Figs. 7(b)-(d). The transverse stress level is relatively low and remains in the elastic stage, while the vertical stress in the steel tubes increases with the loading

due to the bond stresses and frictional forces between the steel plate and the concrete. The increase of transverse stress is accelerated by the expansion of concrete during the plastic stage. After the peak load, the core concrete further expands. The transverse stress of tube keeps increasing, while the vertical stress decreases. At this stage, the main function of tube is to provide lateral confinement to concrete. The stress components at the corners are higher than those at the middle position during the same loading stage, indicating that the concrete is better confined at the corners.

The representative load-stress curves for Specimens SC(GS)-140-2 and SC(GS)-180-2-S are presented in Figs. 7(e)-(h). The stress state of the specimens' square steel tube (Figs. 7(e)-(f)) is similar to that of Specimen S(GS)-200-a because of the similar column failure pattern as described above.

The concrete stress condition at points 8 and 9 of Specimen SC(GS)-140-2, as shown in Figs. 7(h)-(i), maintains at a low level during the entire loading process, indicating that the contribution of RC beams to peak load is small. However, when the beam height increased to 180 mm and stiffening ribs were used (SC(GS)-180-2-S, as

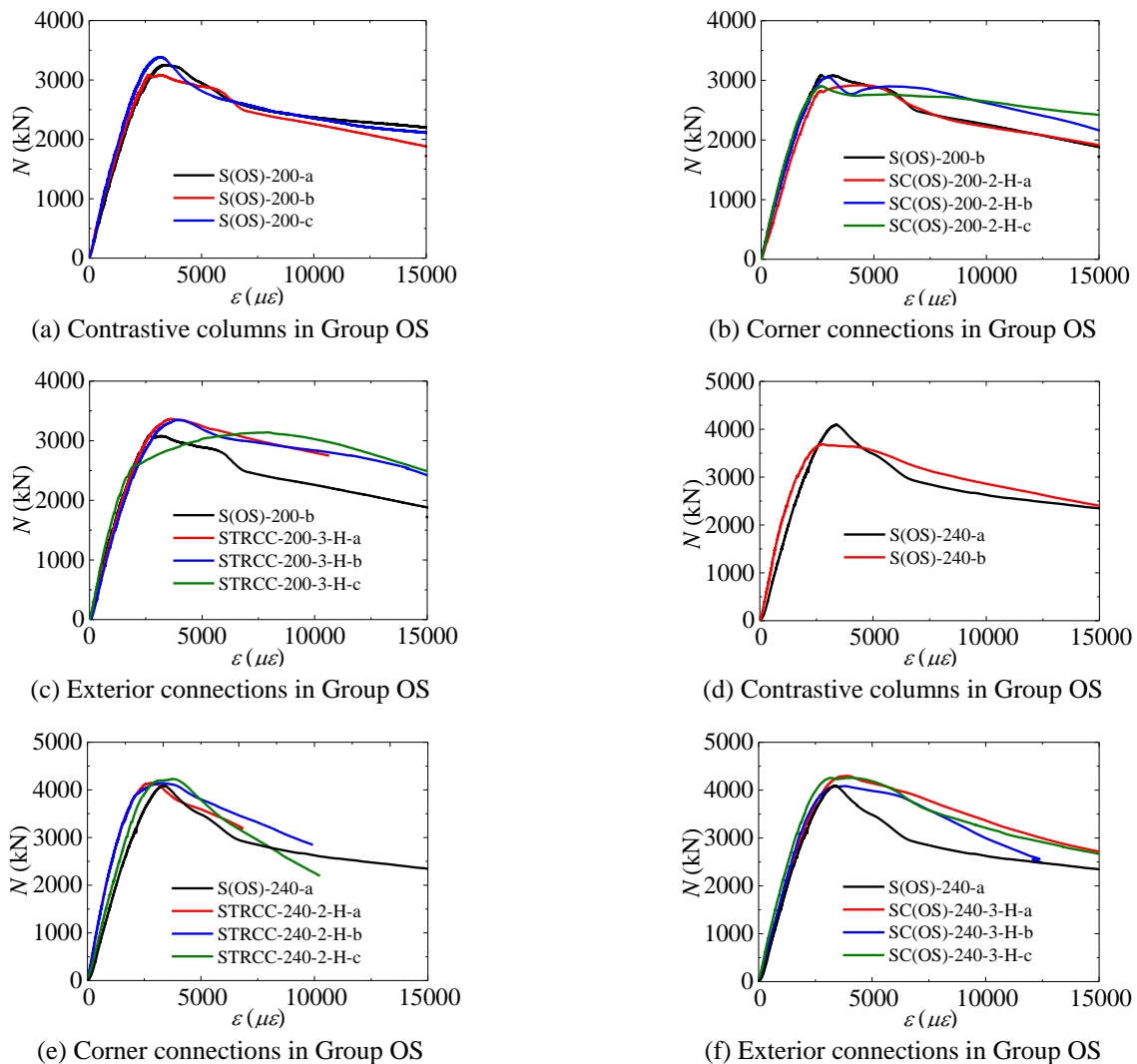
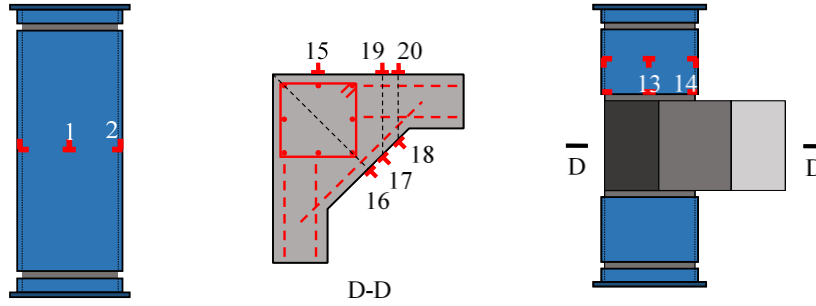
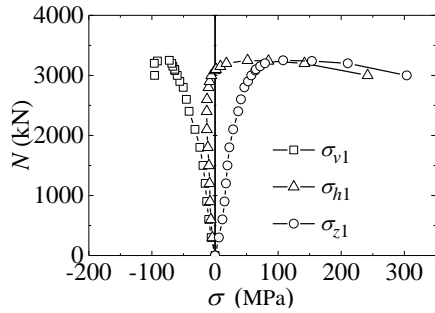


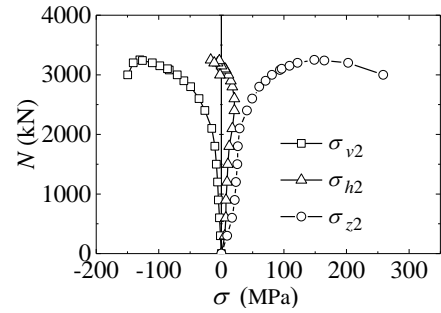
Fig. 9 The load-strain curves of the specimens in Group OS



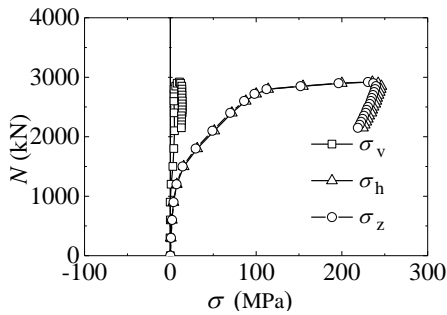
(a) Locations of strain gauges



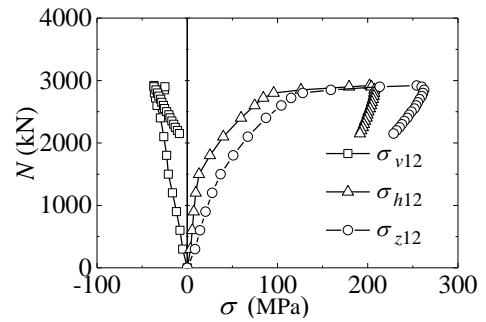
(b) Point 1 of S(OS)-200-a



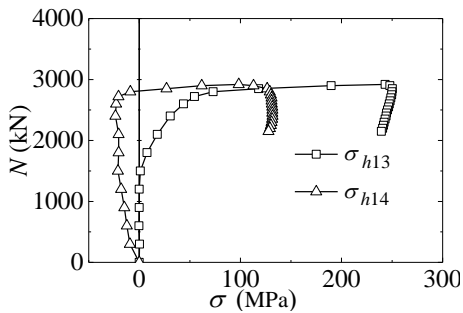
(c) Point 2 of S(OS)-200-a



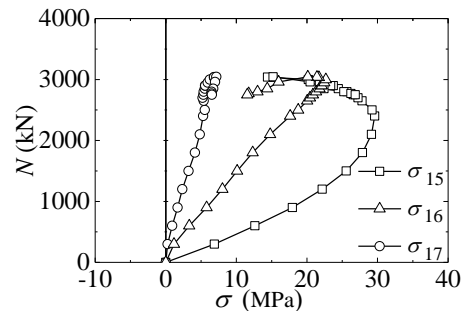
(d) Point 11 of SC(OS)-200-2-H-a



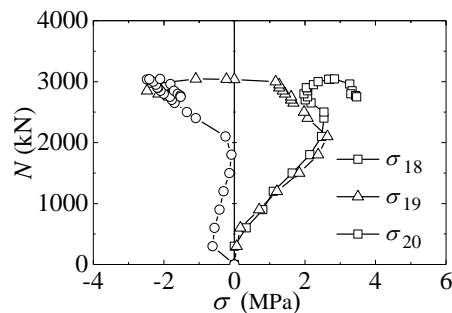
(e) Point 12 of SC(OS)-200-2-H-a



(f) Points 13 and 14 of SC(OS)-200-2-H-a



(g) Points 15 to 17 of SC(OS)-200-2-H-b



(h) Points 18 to 20 of SC(OS)-200-2-H-b

Fig. 10 The load-stress curves of the specimens in Group GS

shown in Fig. 7(i)), the vertical stress at points 8 and 9 increases linearly with the increase of axial loads. This is because the stiffening ribs improve the confinement in the column zone and the higher height (180 mm) of beam section leads to weaker confinement in the joint zone, causing the concrete stress trajectory to spread from joint zone to beam zone. The above analysis results indicate that the contribution of RC beams to peak load depends on the ratio of column resistance to joint zone resistance being influenced by stiffening ribs and the height of joint zone.

4. Test results of Group OS

4.1 Failure patterns

As shown in Figs. 8(a)-(f), the failure patterns of the columns and connections in Group OS are similar to those in Group GS. The failure pattern of the connections in Group OS is typically characterized by the concrete crushing along a diagonal section in the column zone, implying a column failure. Spalling of concrete cover in the vicinity of the joints for the exterior connections was observed due to the nonexistence of transverse RC beams.

4.2 Load-deformation relationship

The load (N)-axial strain (ϵ) curves of the specimens in Group OS are shown in Figs. 9(a)-(f). The peak load of the connection specimens is close to that of the contrastive columns due to the similar column failure. Either connection type or beam height influences little on the peak load. Compared with the corner connections, the exterior connections display a better ductility due to the larger area of horizontal RC haunches.

4.3 Load-stress analysis

Representative load-stress curves for Specimens S(OS)-200-a, SC(OS)-200-2-H-a, and SC(OS)-200-2-H-b are shown in Fig. 10. Since the failure pattern of the connections is characterized by column failure, the load-stress curves of steel tubes are similar to that of the contrastive columns. Namely, the vertical stress of tubes maintains at a relatively low level during the test, while the transverse stress increases sharply due to the expansion of core concrete around the peak load (Figs. 10(b)-(e)). A higher transverse stress at the corner indicates that the confinement effect of square tubes is mainly provided by the arch action at the corners (Fig. 10(f)).

The load-concrete stress relationships of the joint zone are shown in Figs. 10(g)-(h). Further away from the center of column, the vertical compressive stress becomes smaller (points 15, 16 & 17). The concrete away from the concrete core provides the confinement to the joint region as evidenced by the tension stress in that region (e.g., points 19 & 20).

5. Comparison and discussion

The failure pattern of square TRC connection is determined by the peak load of both column zone and joint

zone. If the joint zone has higher peak load, then column failure occurs, or vice versa. The axial bearing capacity of column zone is also weakened due to the steel discontinuity as shown in Table 1. Although the peak load of some connections is lower than that of the corresponding columns. However, this will not change the failure mode because the peak load of joint zone is relatively high compared to column zone in a same specimen.

In this paper, the feasibility of RC beam to square TRC column connection is verified experimentally and analytically. The test results indicate that all the connections including those with stiffened columns are characterized by column failure. The possible decrease of axial resistance due to the discontinuity of column tube can be compensated by using transverse beams, horizontal haunches, and stirrups. The beam height is less than the column width and hence the potential decrease of axial bearing capacity is relatively small; the width to thickness ratio of square tube is 133-160 and thus the confining stress to the column is manageable. As long as the beam height is less than the column width and the width to thickness ratio of steel is greater than 133, the confining stress in joint zone provided by the steel tube is high enough to protect the specimen from joint failure. With a proper design, the axial peak load of the joint zone is expected to be higher than that of the TRC column.

From the test results of the specimens in Group GS, stiffening ribs can significantly improve the load-carrying capacity and ductility. The peak load of the connections with stiffening ribs is 8.6-13.2% higher than that of the connections with no stiffening ribs.

The transverse beam and RC horizontal haunches can improve the ductility and axial load-carrying capacity of the connections. However, due to the lack of protection from transverse beams and RC horizontal haunches, the concrete cover on the exterior faces of exterior and corner joint spalls off in both Group GS and Group OS specimens. The concrete cover at the corner connections in Group OS spalls off seriously due to the offset of the centroid of haunched connection.

All tested connections described in this paper are characterized by column failure under axial compressive loading. However, this phenomenon may not be true under other type of loads such as an earthquake, which needs to be investigated further.

6. Conclusions

Based on the experimental investigation and theoretical analysis, the following conclusions are drawn:

- When the height of RC beam section is less than the width of column, the width to thickness ratio of steel tube is greater than 133, the axial bearing capacity of the proposed RC beam to square tube-reinforced-concrete column connection is higher than that of the contrastive tube-reinforced concrete column. So, with a proper design, this type of connections is feasible to be implemented in real structures.
- Stiffening ribs can significantly improve the load-carrying capacity and ductility of the proposed

connection type.

- The RC horizontal haunch can also improve the ductility and axial load-carrying capacity of both exterior and corner connections.

Acknowledgments

The authors greatly appreciate the financial supports provided by the National Natural Science Foundation of China (No. 51308051, No. 51438001), the Fundamental Research Funds for the Central Universities (No. 106112014CDJZR200004) and Natural Science Basic Research Plan in Shaanxi Province of China (Program No. 2014JQ7249). The opinions expressed in this paper are solely of the authors.

References

- Bai, Y., Nie, J.G. and Cai, C.S. (2008), "New connection system for confined concrete columns and beams. II: Theoretical modeling", *J. Struct. Eng., ASCE*, **134**(12), 1800-1809.
- Chen, S.J., Yang, K.C., Lin, K.M. and Wang, C.D. (2011), "Seismic behavior of ductile rectangular composite bridge piers", *Earthq. Eng. Struct. D.*, **40**(1), 21-34.
- Chen, S.J., Yang, K.C., Lin, K.M. and Wang, C.D. (2012), "Experimental studies of circular composite bridge piers for seismic loading", *Steel Compos. Struct., Int. J.*, **12**(3), 261-273.
- Chen, Q.J., Cai, J., Bradford, M.A., Liu, X. and Zuo, Z.L. (2014), "Seismic behavior of a through-beam connection between concrete-filled steel tubular columns and reinforced concrete beams", *Eng. Struct.*, **80**, 24-39.
- Chen, Q.J., Cai, J., Bradford, M.A., Liu, X. and Wu, Y. (2015), "Axial compressive behavior of through-beam connections between concrete-filled steel tubular columns and reinforced concrete beams", *J. Struct. Eng., ASCE*.
DOI: 10.1061/(ASCE)ST.1943-541X.0001249
- Han, L.H., Qu, H., Tao, Z. and Wang, Z.F. (2009), "Experimental behavior of thin-walled steel tube confined concrete column to RC beam joints under cyclic loading", *Steel Constr.*, **47**(47), 847-857.
- Liu, J.P. and Zhou, X.H. (2010), "Behavior and strength of tubed RC stub columns under axial compression", *J. Constr. Steel Res.*, **66**(1), 28-36.
- Liu, J.P., Zhang, S.M., Zhang, X.D. and Guo L.H. (2009), "Behavior and strength of circular tube confined reinforced-concrete (CTRC) columns", *J. Constr. Steel Res.*, **65**(7), 1447-58.
- Liu, J.P., Wang, X.D. and Zhang, S.M. (2015), "Behavior of square tubed reinforced-concrete short columns subjected to eccentric compression", *Thin Wall. Struct.*, **91**, 108-115.
- Nie, J.G., Bai, Y. and Cai, C.S. (2008), "New connection system for confined concrete columns and beams. I: Experimental study", *J. Struct. Eng., ASCE*, **134**(12), 1787-1799.
- Sakino, K. and Sun, Y.P. (2000), "Steel jacketing for improvement of column strength and ductility", *Proceedings of the 12th World Conference on Earthquake Engineering*, Auckland, New Zealand, January.
- Tomii, M., Sakino, K., Xiao, Y. and Watanabe, K. (1985), "Earthquake resisting hysteretic behaviour of reinforced concrete short columns confined by steel tube", *Proceedings of the International Speciality Conference on Concrete Filled Steel Tubular Structures*, Harbin, China, August.
- Wang, X.D., Liu, J.P. and Zhang, S.M. (2015), "Behavior of short circular tubed-reinforced-concrete columns subjected to eccentric compression", *Eng. Struct.*, **105**, 77-86.
- Yu, Q., Tao, Z., Liu, W. and Chen, Z.B. (2010), "Analysis and calculations of steel tube confined concrete (STCC) stub columns", *J. Constr. Steel Res.*, **66**(1), 53-64.
- Zhang, S.M., Guo, L.H., Ye, Z.L. and Wang, Y.Y. (2005), "Behavior of steel tube and confined high strength concrete for concrete-filled RHS tubes", *Adv. Struct. Eng.*, **8**(2), 101-116.
- Zhang, Y.F., Zhao, J.H. and Cai, C.S. (2012), "Seismic behavior of ring beam joints between concrete-filled twin steel tubes columns and reinforced concrete beams", *Eng. Struct.*, **39**, 1-10.
- Zhou, X.H. and Liu, J.P. (2010), "Seismic behavior and shear strength of tubed RC short columns", *J. Constr. Steel Res.*, **66**(3), 385-397.

BU